Tribol Lett (2016) 64:26
DOI 10.1007/s11249-016-0757-9

ORIGINAL PAPER

Tribological and Sealing Performance of Laser Pocketed Piston Rings in a Diesel Engine

Cong Shen[1] · **M. M. Khonsari**[1]

Received: 11 July 2016 / Accepted: 12 September 2016 / Published online: 1 October 2016

Abstract The tribological and sealing performance of a piston ring with specially designed textured surface in a diesel engine are investigated experimentally. For this purpose, a motorized engine test rig is used to assess the frictional characteristics of compression piston rings with surface-texture pockets with optimum geometries fabricated on their surfaces. Experimental results show that lasered pockets led to a reduction of up to about 15 % in the total friction between cylinder liner and piston assembly over a wide range of operating speed. Further, the results of compression tests with pocketed textures show a slight improvement in the sealing performance compared to untextured piston rings.

Keywords Piston ring · Laser surface texturing · Power loss · Lubrication optimization · Compression sealing

1 Introduction

Surface texturing has emerged as a viable technique for improving the tribological performance of many vital mechanical components, such as mechanical face seals, bearings, cutting tools and even artificial hip joints [1–8]. With stringent requirements on the efficiency and emission of internal combustion engines, there is a heightened need for reducing friction losses in an engine, particularly at the interface between piston rings and cylinder liners. As a result, the application of surface texturing to the piston ring/cylinder liner contact has received increasing attention in recent years [9–20].

One of the early experimental studies on the textured piston rings was carried out by Ryk et al. [9]. They designed a reciprocating test rig to measure the friction between two production piston ring segments and a segment of a cylinder liner with controlled lubricant feeding rate. Based on the results of a theoretical modeling, they fabricated dimples with a diameter of 100 μm, depth of 10 μm and area ratio of 20 % on the surface of piston ring segments. A friction reduction from 20 to 30 % due to texturing was observed in their experiments. In a subsequent work [10, 11], they proposed a design of partial laser surface texturing for piston rings where textures were fabricated on only a portion of the ring face and evaluated its effect on the friction reduction. The comparison of frictional performance was made between cylindrical shape rings with partial texturing and non-textured barrel face rings. It was reported that cylindrical face rings with partial surface texturing can lead to a friction reduction of up to 25 %. Later, actual engine tests with a dynamometer were conducted by Etsion and Sher [12] to compare the fuel efficiency and exhaust gas composition of engines using partially textured piston rings and non-textured barrel-shaped piston rings. They found that optimum partial surface texturing resulted in a reduction of up to 4 % in fuel consumption but had no significant influence on the exhaust gas composition. Bolander and Sadeghi [13] also modified the piston ring surface by laser texturing and compared the performances of circular dimples with different dimensions (dimple diameter and depth). Their experimental results showed that textured piston rings with shallow dimples exhibit lower friction on a polished liner segment. In a recent study by the present authors [20], a

✉ M. M. Khonsari
khonsari@me.lsu.edu

[1] Department of Mechanical and Industrial Engineering, Louisiana State University, 3283 Patrick Taylor Hall, Baton Rouge, LA 70803, USA

new design of surface modification was proposed for the piston ring surface in which micro oil pockets were created at the inlet and outlet of the ring face. During the reciprocating motion, the pockets at the leading edge can function as tiny step bearings and hence generate hydrodynamic pressure to improve the lubrication. A series of experiments were performed to investigate the geometric parameters (area ratio, depth, and shape) of the pockets on the tribological performance of piston ring prototypes. It was found that the pockets with appropriate size can greatly lower the friction at the piston ring/cylinder liner contact.

In most of the previous experimental work on textured piston rings, a reciprocating test rig is utilized to measure the friction between the piston ring segments and cylinder liner segment wherein the ring specimens are affixed to a holder and kept stationary while the cylinder liner is set in reciprocating motion. This test configuration oversimplifies the motion of piston rings and does not account for the secondary motion of piston and piston rings (radial motion, elastic deformation, and twist) in a cylinder, which could have a significant influence on the piston ring lubrication [21]. Clearly, a motorized engine test that employs a piston and a piston ring-pack is desirable for evaluation of textured piston rings, for it can more realistically represent the piston ring motion and lubrication in an actual engine. Moreover, the sealing performance of textured piston ring should also be assessed since the primary function of piston rings is to form a moving seal between the piston and cylinder wall. If the design of surface texturing reduces the sealing capability of piston rings, it would increase the blow-by and lubricant consumption and decrease the engine efficiency, thus limiting the effectiveness of textures in terms of improving engine performance.

In the present study, a motorized engine testing apparatus is employed to evaluate the frictional and sealing performance of piston rings. The motor reciprocates a production piston and piston ring-pack within the cylinder liner of a diesel engine. The results of series of friction and compression pressure tests are presented that compare the performance of flat and pocketed piston rings.

2 Experiment

2.1 Description of Experimental Apparatus

The experiments were conducted using a custom-built reciprocating piston test apparatus that enables both friction and compression pressure measurements. This test apparatus applies the floating liner method [22, 23] to directly measure the piston friction and utilizes the cylinder liner, piston, piston rings and connecting rod from a diesel engine (Perkins 4.236). The reason for using piston rings from a diesel engine is that their axial ring width is larger than those from a gasoline engine. So, relatively large pockets can be created on the ring surface in order to make the effects of lasered pockets more measurable and to make the fabrication easier. Further, the ring tension force and the number of compression rings are greater in a diesel engine. This can lead to a higher and more noticeable piston ring friction.

Figure 1 shows the schematic of the machine. The reciprocating motion of the piston assembly is achieved with an electric motor driving the crankshaft through a set of pulleys. The pulley drive ratio is 3.4:1, and the large pulley connected to the crankshaft can work as a flywheel to ensure smooth motion of the piston. The stroke length used in the study is 114.3 mm, which is similar to that in a typical engine. The rotating speed and angular position of the crankshaft are recorded by a rotary encoder, attached to the end of the crankshaft.

The test apparatus has two configurations for the cylinder liner: a suspended configuration for measuring the friction force and a fixed configuration for measuring the compression pressure. During the friction tests, the cylinder liner is suspended by a load cell to measure the axial friction force, as shown in Fig. 2a. The radial motion of the cylinder liner is prevented by three lateral supports positioned at 120° spacing. Each lateral support is equipped with two ball bearings that maintain the center position of the liner and accommodates smooth motion in the axial direction. The weight of the cylinder liner and its fixture is counterbalanced by a lever and weight assembly to eliminate its influence on the friction measurement. The cylinder liner is open at its end without a cylinder head in the friction tests so that the compression gas is not sealed and the friction is the only force acting on the suspended liner.

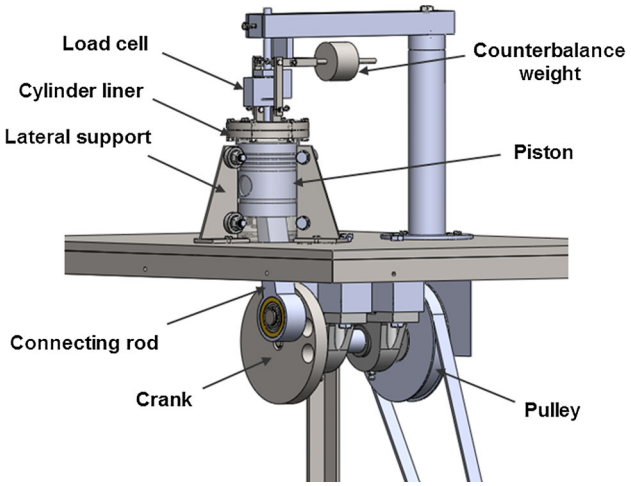

Fig. 1 Schematic of the test rig

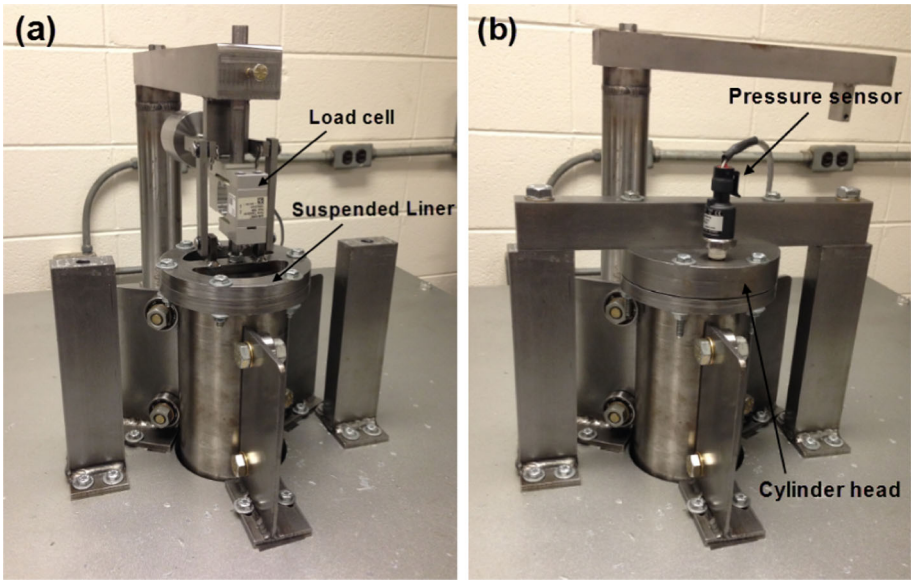

Fig. 2 Final assembly of the test rig: **a** suspended-liner configuration for friction test; **b** fixed-liner configuration for compression pressure test

In the compression pressure tests, the cylinder liner is sealed with a cylinder head and a gasket. Due to the high-pressure loading, the liner is fixed to a support bar, as shown in Fig. 2b. The lateral force acting on the liner is also balanced by three lateral supports. A pressure transducer (with a range of 1.38 MPa and accuracy of 1 %) is inserted through the cylinder head to monitor the pressure variation inside the cylinder liner.

Figure 3 shows the lubrication arrangement of the test rig. The lubricating oil is sprayed to the bottom of the piston and cylinder liner by using a nozzle connected to the oil circulation system. Some of the lubricant could flow through the holes in the piston to the cylinder wall and then be regulated by the oil control rings. This is very similar to the lubricant flow in a real engine. The lubricant oil is stored in an oil tank, equipped with a heater and a temperature control, and pumped through a filter. An oil catcher collects the lubricant that falls out of the cylinder liner and drains it back to the tank. The oil flow rate is controlled by a valve available next to the gear pump and monitored by a flowmeter.

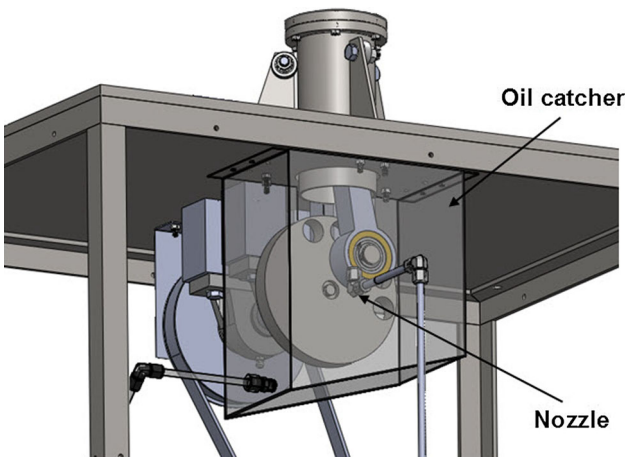

Fig. 3 Lubrication arrangement of the test rig

All measurement data (including the data from the rotary encoder, load cell, pressure transducer and the thermocouple in the oil tank) are acquired with a data acquisition system and a LabVIEW program. This program is also capable of real-time data processing for reducing noise in the signal. It needs to be noted that a motorized engine test rig cannot simulate strictly identical operating conditions of a fired engine. It does not account for the effects of high combustion pressure and high temperature. During the power stroke, the compression pressure in the combustion chamber increases dramatically, leading to a much higher loading on the piston rings and a more severe lubrication condition. The heat generated during combustion increases the lubricant temperature and hence reduces its viscosity. Nevertheless, friction testing with a fired engine has considerable difficulties and requires substantial engine modification, while motorized engine tests can eliminate many of these complications. Moreover, Mufi and Priest [24] have shown that if the high temperature is maintained in a motorized test, the total friction measured is very close to that of the fired conditions, except during power stroke. The effects of surface texturing on the power gain under fired engine tests were investigated by Howell-Smith, et al. [25], and interested readers are referred to their work for more details.

2.2 Specimen Preparation

The piston ring-pack used in this study consists of three compression rings and two oil control rings. The micro

pockets were machined on the sliding surface of the compression rings made of cast iron with a diameter of 99 mm and a width of 2.36 mm. All the compression rings have a flat surface with a surface roughness (R_a) of 0.32 μm.

A Nd:Ytterbium fiber laser (wavelength of 1064 nm) is used to fabricate micro pockets on the piston ring surface. The shape and distribution of the pockets are first designed using a CAD software and then imported into the laser device. The pocket depth is controlled by the power of the laser and the number of repeats the laser beam scans the surface. Figure 4 shows the surface of a laser pocketed compression ring. The geometric parameters of the pockets are listed in Table 1. These dimensions are selected based on a previous study [20] that identified the optimal range of the pocket size. A trapezoid shape is used in the design of pockets since it has been proved to be an optimum shape for two-dimensional slider bearings [26, 27]. Here the pocket depth is slightly shallower than the previous study because the piston ring/cylinder liner contact is not operating under submerged lubrication and the lubricant film thickness is expected to be lower than that in previous tests.

2.3 Experimental Procedure

Two types of experiments were performed: friction tests and compression pressure tests. Each piston ring-pack underwent both tests. The adjustable parameters in the experiments include: crank rotational speed, oil temperature (viscosity), oil supply rate and surface finish of the compression rings. In this study, the rotational speed was varied from 60 to 600 rpm. Testing at higher speeds would be affected by the test rig vibration and require an ultra-high sampling rate. Also, preliminary tests have shown that the general trend of friction traces does not change if the speed is further increased. An additive-free SAE 30 oil was used in the tests, and its bulk temperature was precisely controlled. Figure 5 shows the dynamic viscosity of the oil as a function of temperature. In order to evaluate the effect of lubricant viscosity, the friction tests were conducted at temperatures of 25 and 60 °C, which corresponds to dynamic viscosities of 0.17 and 0.03 Pa s. The oil flow rate was maintained at 1.2 L/min for all the experimental tests.

The test procedure for friction measurement is as follows. First, the weight of cylinder liner and its fixture was balanced by adjusting the position of the counterbalance weight. Then, the piston rings were installed in the test rig and the gear pump of the lubricant circulation system was turned on. After a running-in process of 6 h, the friction tests were performed under various crank speeds ranging from 60 to 600 rpm. Friction data of 100 reciprocating cycles were collected for each test condition with 1000 data points per cycle, and a low pass filter was applied to reduce high-frequency noise in the signal. The averaged friction force is used to represent the result of each test. It is calculated by averaging the absolute values of the friction force over 100 reciprocating cycles. Minimum of three non-consecutive tests were conducted for each test condition and their friction variations were compared to ensure the measurement consistency. Figure 6 shows the friction force history of three tests. Good repeatability and stability were observed in the test results.

After the friction tests, the compression pressure tests were conducted with the same piston ring-pack at room temperature (25 °C). A cylinder head and a gasket were installed to form a compression chamber. The rotational speed of the crank was set to 120, 180, 240 and 360 rpm in the compression tests. The oil flow rate and data sampling

Table 1 Geometric parameters of lasered pockets

Parameters	Value
Pocket shape	Trapezoidal
Characteristic length	$a = 0.6$ mm; $b = 0.36$ mm; $h = 0.75$ mm
Pocket depth	3.9–4.2 μm
Pocket spacing	2.8° (circumferentially)
Total no. of pockets	516
Area ratio	25.3 %

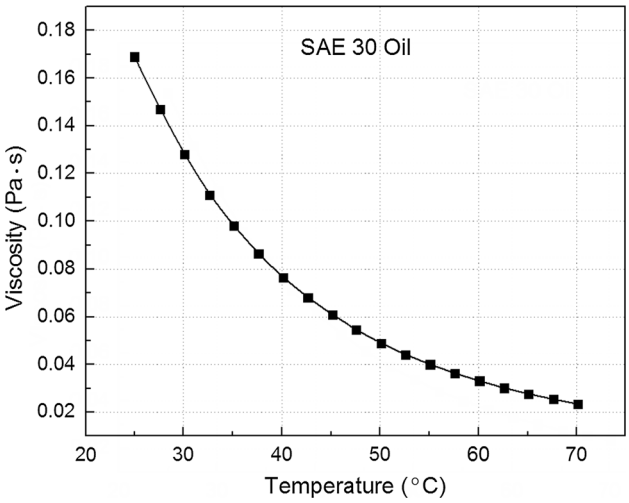

Fig. 5 Dynamic viscosity of the lubricant oil as a function of temperature

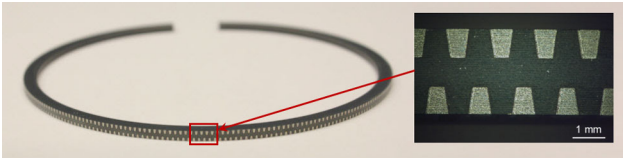

Fig. 4 Image of pocketed compression ring

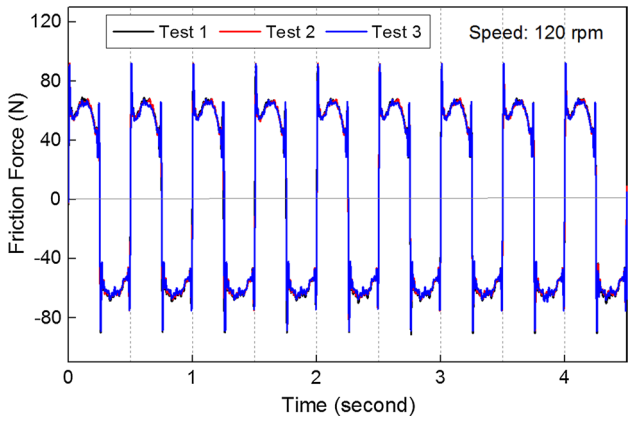

Fig. 6 Friction force variation versus time for three friction tests of the smooth rings

rate were the same as those in the friction tests. The pressure variation in the reciprocating cycles was recorded with a pressure transducer. The peak pressure of 100 cycles was averaged and used to evaluate the sealing performance of piston rings.

3 Results and Discussion

3.1 Friction Test Results

Figure 7 presents the average friction force versus the crank rotational speed for both smooth and pocketed piston rings. As can be seen, the average friction shows a persistent increase in the increasing crank speed. The measured friction consists of contributions from each piston ring and the piston skirt, and the friction force acting on each part includes a viscous shear force in the lubricant film and friction from contacting asperities. An increase in

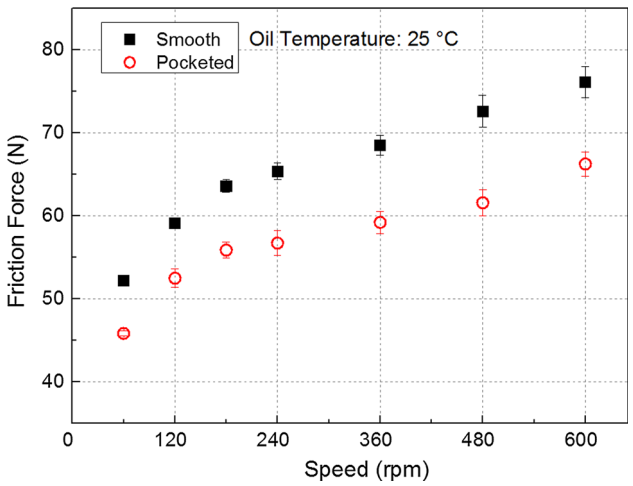

Fig. 7 Comparison of averaged friction force at oil temperature of 25 °C

the speed would improve the hydrodynamic action, leading to increased fluid film separation and hence reduced asperity contact and friction. On the other hand, the viscous shear force would increase with the sliding speed, since it is proportional to the shear rate and viscosity. These two competing factors influence the total measured force. The trend of increased friction with speed indicates that the increase of viscous force is more dominant in the total friction.

Comparing with the smooth piston rings, the pocketed rings have a consistently lower value of averaged friction over the entire speed range. The friction reduction resulted from the lasered pockets is varied from 11 to 15 % of the total friction. The mechanism for the reduced friction is thought to be different depending on the operating conditions. The lubrication arrangement in this study is similar to that of a real engine. Excess oil on the cylinder wall drains into the oil catcher due to gravity and is also wiped off by the oil control ring, leaving only a thin layer of oil retained on the surface to provide lubrication. As a result, there would be a certain degree of oil starvation at the piston ring/cylinder liner interface, especially when the rotational speed is low and oil cannot be splashed onto the cylinder wall. A possible reason for the friction reduction of pocketed rings at low speed is that these pockets can act as oil reservoirs during sliding, thus help to supply oil to the contact surface and reduce asperity contacts. This is similar to the effects of surface texturing of liner surface during reversals, and the pressure perturbations at the inlet due to surface texturing could also contribute to the reduction of friction [28]. However, at high speeds where the hydrodynamic action is more dominant, the pockets are expected to work as tiny step bearings and generate additional hydrodynamic pressure and load-carrying capacity. The influence of lasered pockets on the load-carrying capacity of piston rings has been analyzed numerically in a previous study [20]. Due to the above two mechanisms, the pocketed rings exhibits better performance over a wide speed range.

Figure 8 illustrates the friction test results with SAE 30 oil at 60 °C. As the oil temperature is increased from 25 to 60 °C, its viscosity drops from 0.17 to 0.03 Pa s. Comparing with Fig. 7, it can be seen that the magnitude of average friction is reduced at an oil temperature of 60 °C, especially at high speeds. This is attributed to the reduction of viscous shear force by the decrease in the lubricant viscosity. The friction reduction effect of the lasered pockets is also observed with a higher oil temperature (lower oil viscosity), and it is more noticeable at low speeds than at high speeds. This behavior can be explained by the friction reduction mechanism of the pockets. As the oil temperature is increased, the fluidity of the oil increases and the oil can flow off or get wiped off the cylinder wall

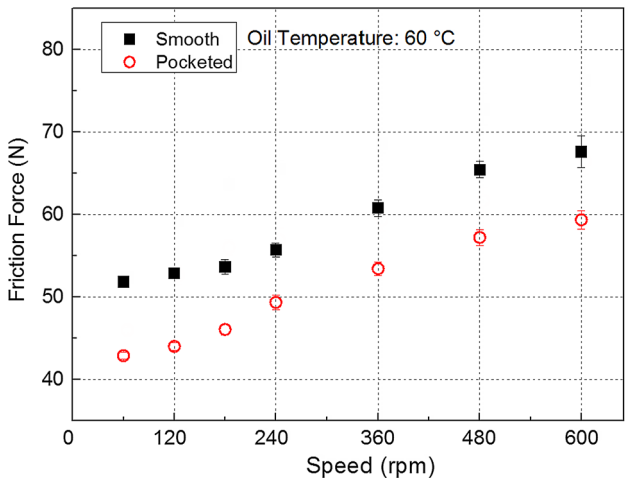

Fig. 8 Comparison of averaged friction force at oil temperature of 60 °C

more easily. This would increase the degree of oil starvation at the piston ring/cylinder liner contact under low speeds and make the oil-reservoir effect of the pockets more distinct at low speeds. On the other hand, the hydrodynamic lift generated by the pockets at high speeds could decrease due to a lower oil viscosity, leading to reduced effects of pockets at high speeds.

Figure 9 shows typical friction force variation over two reciprocating cycles. As the speed is increased from 60 to 480 rpm, the friction force exhibits different trends. Under low speeds (60 rpm), the friction force reaches its highest value at the beginning and end of the reciprocating strokes (top and bottom dead centers), where the sliding velocity is the lowest and the friction is dominated by asperity contacts. Increasing the crank speed to 120 and 240 rpm results in lower friction spikes at dead centers and friction starts to build-up around mid-stroke. This trend is attributed to increased hydrodynamic action at the piston ring/cylinder liner interface and the rise in viscous shear force due to higher sliding speeds. Further increase in the crank speed to 480 rpm leads to a friction trace with a sinusoidal shape. The asperity interaction is greatly reduced near the dead centers, and the friction force has its

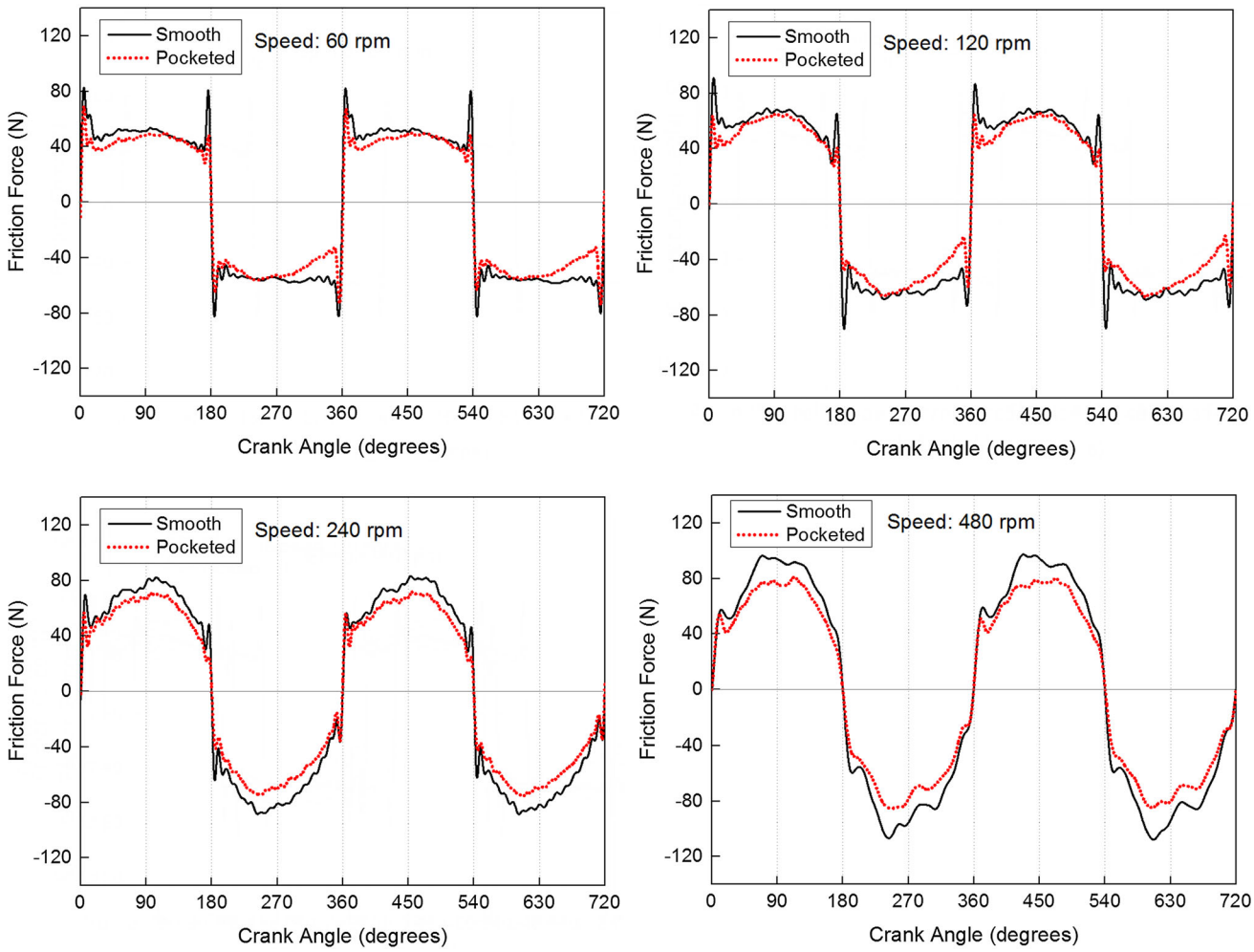

Fig. 9 Friction force variation over two reciprocating cycles at oil temperature of 25 °C

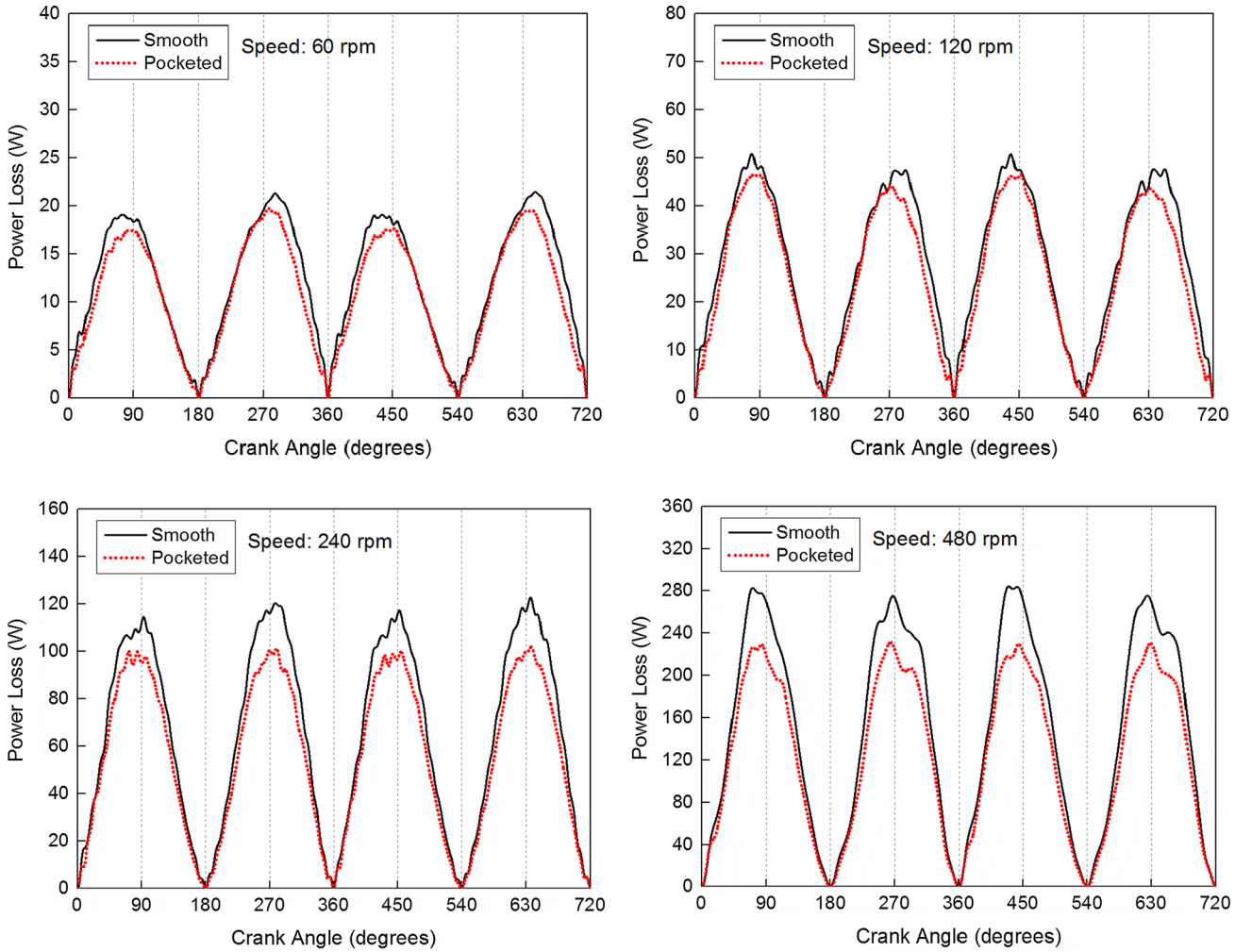

Fig. 10 Power loss variation over two reciprocating cycles at oil temperature of 25 °C

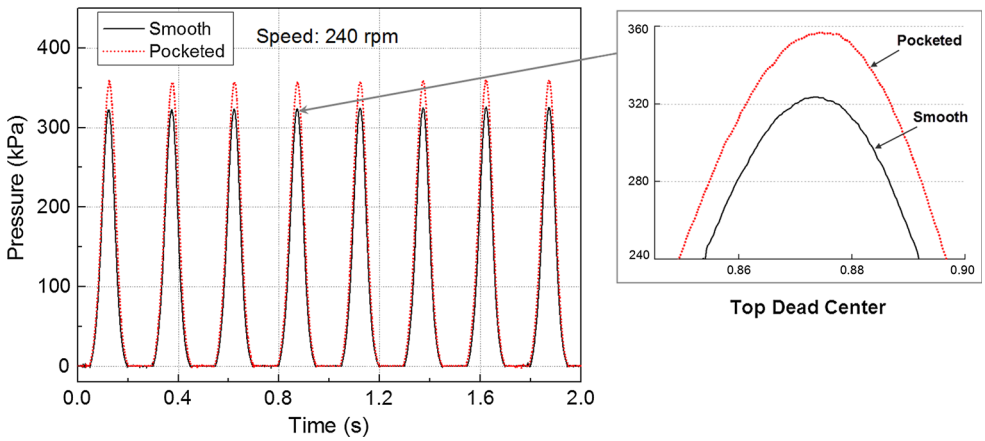

Fig. 11 Chamber pressure variation at the speed of 240 rpm

highest value in the middle of the stroke, where the sliding velocity is maximum throughout the reciprocating cycle. This indicates that the viscous shear force is dominant in the total friction under high speeds. Since shear force is proportional to the shear rate (sliding speed divided by the film thickness), a higher speed usually results in a higher viscous force, although film thickness could also increase with speed but this effect is less significant than the impact of increased speed. The change of friction trace shape due to the crank speed is similar to that observed in Ref. [29].

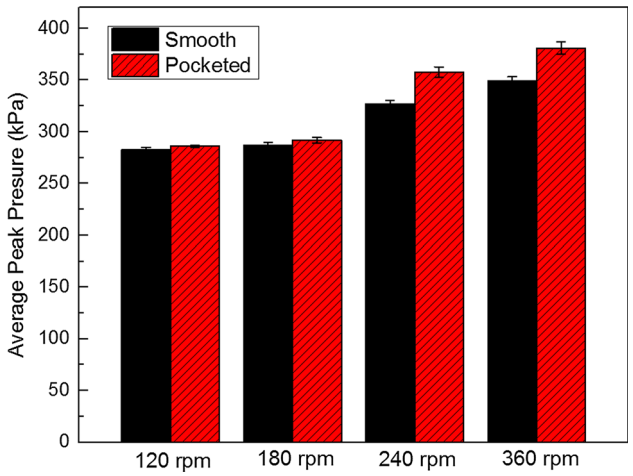

Fig. 12 Comparison of averaged peak pressure

Comparison of the friction traces for smooth and pocketed piston rings show that the friction reduction effects of the pockets vary depending on the operating conditions. At lower speeds, their major effect is to reduce the friction spikes near the dead centers. A major reason for the friction spikes is the lubrication starvation. The piston ring sliding velocity approaches zero near the dead centers and hence there is a momentary cessation of the oil entrainment into the contact. Moreover, the cavitation region in the outlet of the piston rings becomes its inlet at the reversals (dead centers), which could cause further starvation effect [30]. As a result, the oil-reservoir function of the pockets can greatly improve piston ring lubrication in this portion of stroke and reduce the magnitude of friction peaks. However, at higher speeds, the pockets can help lower the magnitude of the hump in the friction trace that occurs around the mid-stroke. This effect can be explained by additional load-carrying capacity generated by laser pockets, which could help increase the lubricant film thickness and reduce the viscous force. Figure 10 shows the corresponding friction power losses of the piston assembly during two reciprocating cycles. As can be seen, the effects of lasered pockets on the power loss is more pronounced at high crank speeds (240 and 480 rpm). The reason is that power loss is a function of both friction and sliding velocity. The maximum power loss usually occurs around the mid-stroke as the piston reaches its maximum velocity near the mid-stroke. When the crank speed is low, the major friction reduction of the pockets occurs near the dead centers, where the sliding velocity is lowest. As a result, the influence of pockets on the power loss is minor at low speeds. However, when the crank speed is high, the peak friction is shifted to the mid-stroke and friction reduction of the pockets also concentrates on that portion, leading to a more significant reduction in the friction power loss.

3.2 Compression Test Results

Compression pressure tests were performed to evaluate the effects of lasered pockets on the sealing performance of piston rings. The sealing functions of piston rings are twofold: (a) sealing the high-pressure gas in the combustion chamber, and (b) regulating the amount of oil on the cylinder wall. It is desirable to investigate the effects of lasered pockets on the oil flow through the ring. But since the rate of oil flow entering the ring pack is very small and the oil on the cylinder wall keeps flowing due to gravity, it is difficult to measure the amount of oil flow accurately. Hence, this study focuses on the gas-sealing function of the piston rings, which has a direct influence on the engine output power and fuel efficiency.

The cylinder pressure was measured with a pressure transducer at crank speeds of 120, 180, 240 and 360 rpm. For each test condition, the cylinder pressure was recorded for 100 cycles with 1000 data points per cycle. Figure 11 shows a typical pressure variation of both smooth and pocketed piston rings. The peak cylinder pressure occurs around the top dead center and its value is extracted from the pressure traces to assess the sealing performance. Figure 12 shows the averaged peak pressure of 100 cycles for smooth and pocketed piston rings. As can be seen, the peak pressure of the pocketed piston rings is consistently higher than that of the smooth rings. This suggests that the lasered pockets do not have detrimental effects on the gas sealing performance of the piston rings. In fact, they could improve the cylinder's compression to some extent. One possible reason for that is the oil stored in the pockets can be supplied to the contact surface under starved lubrication and fill some of the gap between the piston ring and cylinder wall, which helps to improve the sealing at the interface.

4 Conclusions

An experimental study was performed to investigate the effect of lasered pockets on the frictional and sealing performance of production piston rings. The piston ring set, piston, cylinder liner and connecting rod from a diesel engine were utilized in a newly developed test apparatus for the measurement of friction force and compression pressure. Micro-pockets with optimal geometries were selected based on a previous study and fabricated on the running surface of compression rings using a laser. The friction test results show that lasered pockets lead to a reduction of up to about 15 % in the total friction between cylinder liner and piston assembly over a wide speed range. This effect can be attributed to mechanisms of the pockets which can act as micro oil reservoirs under starved lubrication and work as tiny step bearings under full film

lubrication. The compression pressure test results show that sealing performance of the piston rings was slightly improved.

References

1. Etsion, I., Kligerman, Y.: Analytical and experimental investigation of laser-textured mechanical seal faces. Tribol. Trans. **42**(3), 511–516 (1999)
2. Wang, X., Kato, K.: Improving the anti-seizure ability of SiC seal in water with RIE texturing. Tribol. Lett. **14**, 275–280 (2003)
3. Lu, X., Khonsari, M.M.: An experimental investigation of dimple effect on the stribeck curve of journal bearings. Tribol. Lett. **27**, 169–176 (2007)
4. Tala-Ighil, N., Fillon, M.: A numerical investigation of both thermal and texturing surface effects on the journal bearings static characteristics. Tribol. Int. **90**, 211–219 (2015)
5. Wang, X., Kato, K., Adachi, K., Aizawa, K.: Loads carrying capacity map for the surface texture design of SiC thrust bearing sliding in water. Tribol. Int. **36**, 189–197 (2003)
6. Herry, Y., Bouyer, J., Fillon, M.: An experimental analysis of the hydrodynamic contribution of textured thrust bearings during steady-state operation: a comparison with the untextured parallel surface configuration. Proc. Inst. Mech. Eng. Part J J. Eng. Tribol. **229**, 362–375 (2015)
7. Ling, T.D., Liu, P., Grzina, D., Cao, J., Wang, Q.J.: Surface texturing of drill bits for adhesion reduction and tool life enhancement. Tribol. Lett. **52**, 113–122 (2013)
8. Chyr, A., Qiu, M., Speltz, J.M., Jacobsen, R.L., Sanders, A.P., Raeymaekers, B.: A patterned microtexture to reduce friction and increase longevity of prosthetic hip joints. Wear **315**, 51–57 (2014)
9. Ryk, G., Kligerman, Y., Etsion, I.: Experimental investigation of laser surface texturing for reciprocating automotive components. Tribol. Trans. **45**(4), 444–449 (2002)
10. Ryk, G., Kligerman, Y., Etsion, I., Shinkarenko, A.: Experimental investigation of partial laser surface texturing for piston rings friction reduction. Tribol. Trans. **48**(4), 583–588 (2005)
11. Ryk, G., Etsion, I.: Testing piston rings with partial laser surface texturing for friction reduction. Wear **261**, 792–796 (2006)
12. Etsion, I., Sher, E.: Improving fuel efficiency with laser surface textured piston rings. Tribol. Int. **42**(4), 542–547 (2009)
13. Bolander, N. W., Sadeghi, F.: Surface modification for piston ring and liner. IUTAM Symposium on Elastohydrodynamics and Microelastohydrodynamics, Snidle, R.W., Evans, H.P. (eds.) pp. 271–283. Springer, Amsterdam (2006)
14. Gadeschi, G.B., Backhaus, K., Knoll, G.: Numerical analysis of laser-textured piston-rings in the hydrodynamic lubrication regime. ASME J. Tribol. **134**, 041702 (2012)
15. Tomanik, E.: Modelling the hydrodynamic support of cylinder bore and piston rings with laser textured surfaces. Tribol. Int. **59**, 90–96 (2013)
16. Zavos, A.B., Nikolakopoulos, P.G.: Simulation of piston ring tribology with surface texturing for internal combustion engines. Lubr. Sci. **27**(3), 151–176 (2015)
17. Vladescu, S.C., Medina, S., Olver, A.V., Pegg, I.G., Reddyhoff, T.: Lubricant film thickness and friction force measurements in a laser surface textured reciprocating line contact simulating the piston ring–liner pairing. Tribol. Int. **98**, 317–329 (2016)
18. Vladescu, S.C., Olver, A.V., Pegg, I.G., Reddyhoff, T.: Combined friction and wear reduction in a reciprocating contact through laser surface texturing. Wear **358**, 51–61 (2016)
19. Gu, C., Meng, X., Xie, Y., Fan, J.: A thermal mixed lubrication model to study the textured ring/liner conjunction. Tribol. Int. **101**, 178–179 (2016)
20. Shen, C., Khonsari, M.M.: The effect of laser machined pockets on the lubrication of piston ring prototypes. Tribol. Int. **101**, 273–283 (2016)
21. Taylor, R.I., Evans, P.G.: In-situ piston measurements. Proc. Inst. Mech. Eng Part J J. Eng. Tribol. **218**, 185–200 (2004)
22. Liao, K., Liu, Y., Kim, D., Urzua, P., Tian, T.: Practical challenges in determining piston ring friction. Proc. Inst. Mech. E Part J J. Eng. Tribol. **227**, 112–125 (2012)
23. Gore, M., Theaker, M., Howell-Smith, S., Rahnejat, H., King, P.D.: Direct measurement of piston friction of internal-combustion engines using the floating-liner principle. Proc. Inst. Mech. Eng. Part D J. Automob. Eng. **228**, 344–354 (2014)
24. Mufti, R., Priest, M.: Experimental evaluation of piston assembly friction under motored and fired conditions in a gasoline engine. ASME J. Tribol. **127**, 826–836 (2005)
25. Howell-Smith, S., Rahnejat, H., King, P.D., Dowson, D.: Reducing in-cylinder parasitic losses through surface modification and coating. Proc. Inst. Mech. Eng. Part J J. Eng. Tribol. **228**, 391–402 (2014)
26. Fesanghary, M., Khonsari, M.M.: Topological and shape optimization of thrust bearings for enhanced load-carrying capacity. Tribol. Int. **53**, 12–21 (2012)
27. Shen, C., Khonsari, M.M.: Numerical optimization of texture shape for parallel surfaces under unidirectional and bidirectional sliding. Tribol. Int. **82**, 1–11 (2015)
28. Morris, N., Rahmani, R., Rahnejat, H., King, P.D., Howell-Smith, S.: A numerical model to study the role of surface textures at top dead center reversal in the piston ring to cylinder liner contact. ASME J. Tribol. **138**, 021703 (2016)
29. Cater, M., Bolander, N.W., Sadeghi, F.: A novel suspended liner test apparatus for friction and side force measurement with corresponding modeling. SAE Technical Paper, 2006-32-0041 (2006)
30. Vladescu, S.C., Olver, A.V., Pegg, I.G., Reddyhoff, T.: The effects of surface texture in reciprocating contacts: an experimental study. Tribol. Int. **82**, 28–42 (2015)